Estimating the Adversarial Robustness of Attributions in Text with Transformers

Adam Ivankay, Mattia Rigotti, Ivan Girardi and **Chiara Marchiori**
IBM Research Zurich
Rüschlikon, Switzerland
{aiv,mrg,ivg,chi}@zurich.ibm.com

Pascal Frossard
École Polytechnique Fédérale de Lausanne (EPFL)
Lausanne, Switzerland
pascal.frossard@epfl.ch

arXiv:2212.09155v1 [cs.LG] 18 Dec 2022

Abstract

Explanations are crucial parts of deep neural network (DNN) classifiers. In high stakes applications, faithful and robust explanations are important to understand and gain trust in DNN classifiers. However, recent work has shown that state-of-the-art attribution methods in text classifiers are susceptible to imperceptible adversarial perturbations that alter explanations significantly while maintaining the correct prediction outcome. If undetected, this can critically mislead the users of DNNs. Thus, it is crucial to understand the influence of such adversarial perturbations on the networks' explanations and their perceptibility. In this work, we establish a novel definition of attribution robustness (AR) in text classification, based on Lipschitz continuity. Crucially, it reflects both attribution change induced by adversarial input alterations and perceptibility of such alterations. Moreover, we introduce a wide set of text similarity measures to effectively capture locality between two text samples and imperceptibility of adversarial perturbations in text. We then propose our novel TRANSFORMER-EXPLANATIONATTACK (TEA), a strong adversary that provides a tight estimation for attribution robustness in text classification. TEA uses state-of-the-art language models to extract word substitutions that result in fluent, contextual adversarial samples. Finally, with experiments on several text classification architectures, we show that TEA consistently outperforms current state-of-the-art AR estimators, yielding perturbations that alter explanations to a greater extent while being more fluent and less perceptible.

1 Introduction

Attribution methods aim to give insight into causal relationships between deep neural networks' (DNNs) inputs and their outcome prediction. They are fundamental to unravel the black-box nature of DNNs and are widely used both in the image and natural language domain. Commonly used attributions like Saliency (Simonyan et al., 2013) Integrated Gradients (Sundararajan et al., 2017), DeepLift (Shrikumar et al., 2017) and self-attention (Bahdanau et al., 2014) highlight input features that are deemed important for the DNNs in the inference process.

However, it has been shown recently that these methods do not deliver trustworthy, *faithful* explanations (Ghorbani et al., 2019; Jacovi and Goldberg, 2020). In particular, many of these attributions lack robustness towards small input perturbations. Carefully crafted, *imperceptible* input alterations change the explanations significantly without modifying the output prediction of the DNNs. This violates the *prediction assumption* of faithful explanations (Jacovi and Goldberg, 2020), i.e similar inputs having similar explanations for the same outputs. Figure 1 exemplifies this fragility of attributions in text. In many safety-critical natural language processing problems, such as EHR classification (Girardi et al., 2018), adversarial robustness is a key factor for DNNs to be deployed in real life. For instance, a medical professional assessing EHRs would neither understand nor trust a model that yields two significantly different explanations for seemingly identical input texts and predictions. Hence, it is fundamental to understand how the networks and attributions behave in the presence of input perturbations and how perceptible those alterations are to the user.

In this work, we focus on estimating the adversarial robustness of attribution maps (AR) in *text classification* problems. Specifically, we are interested in investigating and quantifying the extent to

Original sample	TEA perturbed sample (ours)	TEF perturbed sample (Ivankay et al., 2021)
peek at the week : ben vs. the streak | yet another risky game for that patriots winning streak , now at 21 . pittsburgh hasn # 39;t lost at home , and rookie quarterback ben roethlisberger hasn # 39;t lost , period . F($\boldsymbol{s}$, "Sports") = 0.99	peek at the playoffs : ben vs. the steelers | yet another risky game for that patriots winning streak , now at 21 . pittsburgh hasn # 34 lost at home , and rookie quarterback ben roethlisberger hasn # 39;t lost , period $\geq$ F($\boldsymbol{s}$, "Sports") = 0.95 **PCC**: 0.02 *SemS*: 0.97, k: 14.9	hoodwink at the zou : suis vs. the wave | yet another risky game for that patriots winning streak , now at 21 . pittsburgh hasn # 39;t lost at home , and rookie quarterback ben roethlisberger hasn # 39;t lost , period . F($\boldsymbol{s}$, "Sports") = 1.0 **PCC**: 0.22 *SemS*: 0.9, k: 3.4
press the delete key . F($\boldsymbol{s}$, "Negative") = 0.99	hit the delete key . F($\boldsymbol{s}$, "Negative") = 0.95 **PCC**: -0.05 *SemS*: 0.98, k: 30	newspaper the delete key . F($\boldsymbol{s}$, "Negative") = 0.95 **PCC**: 0.6 *SemS*: 0.8, k: 1.1
intel seen readying new wi - fi chips | intel corp . this week isexpected to introduce a chip that adds support for a relativelyobscure version of wi - fi , analysts said on monday , in a movethat could help ease congestion on wireless networks . F($\boldsymbol{s}$, "Sci/Tech") = 0.78	intel seen readying wireless wi - fi chips | intel corp . this week isexpected to launch a specification that added support for a relativelyobscure version of wi - fi , analysts said on monday , in a movethat could help ease congestion on wireless networks . F($\boldsymbol{s}$, "Sci/Tech") = 0.95 **PCC**: 0.27 *SemS*: 0.98, k: 20	intel seen readying nouveau wi - fi chips | intel corp . this week isexpected to insert a dies that summing support for a relativelyobscure version of wi - fi , analysts said on monday , in a movethat could help ease congestion on wireless networks . F($\boldsymbol{s}$, "Sci/Tech") = 0.95 **PCC**: 0.28 *SemS*: 0.91, k: 4

Figure 1: Attribution maps in text sequence classifiers are not robust to word substitutions. By carefully altering the original sample, the perturbed samples result in significantly different attribution maps while maintaining the prediction confidence F in the correct class. Red words have positive attribution values, i.e. contribute *towards* the true class, while blue words with negative attributions *against* it. Our novel TEA attack yields perturbed samples that have lower *Pearson Correlation Coefficient* (PCC) values between the attribution maps of original and perturbed inputs, as well as higher semantic similarity values (SemS) of the original and adversarial sentences, compared to the baseline TEF attack. This results in higher estimated robustness constants k (see Section 4), thus lower robustness of the classifiers against the attack.

which small input perturbations can alter explanations in DNNs and how perceptible such alterations are. Moreover, we focus on methods to find the optimal perturbations that maximize the change in attributions while being as imperceptible as possible. We summarize our contributions as follows:

- We are the first to introduce a definition of attribution robustness (AR) in text classification, derived from the Lipschitz-constant, that takes into account both the attribution distance and perceptibility of perturbations.
- We are the first to propose a diverse set of metrics to capture numerous aspects of perceptibility of small input perturbations in text.
- We introduce a novel and powerful attack technique, TRANSFORMEREXPLANATIONATTACK (TEA), that we show consistently outperforms state-of-the-art adversaries and therefore allows us to more tightly estimate attribution robustness in text classifiers.
- We are the first to utilize masked language models (MLMS) for context-aware candidate extraction in attribution robustness estimation. This is crucial, as domain-specific MLMs are becoming increasingly available, making them a progressively attractive alternative to custom synonym embeddings on which current methods have to rely.
- We successfully speed up robustness estimation with the usage of distilled language models and batch masking.

2 Related work

The robustness aspect of faithful explanations (Jacovi and Goldberg, 2020) has recently been studied

with increasing interest. The authors Ghorbani et al. (2019) were the first to show that attribution methods like Integrated Gradients (Sundararajan et al., 2017) and DeepLift (Shrikumar et al., 2017), amongst others, lack robustness to local, imperceptible perturbations in the input that lead to significantly altered attribution maps while maintaining the correct prediction of the image classifier. The works of Dombrowski et al. (2019), Chen et al. (2019), Moosavi-Dezfooli et al. (2019), Rigotti et al. (2022) and Ivankay et al. (2020) have further studied this phenomenon and established theoretical frameworks to understand and mitigate the lack of attribution robustness in the image domain.

However, explanation robustness in natural language processing has not been explored as deeply. The authors Jain and Wallace (2019) and Wiegreffe and Pinter (2019) show that similar inputs can lead to similar attention values but different predictions, and that models can be retrained to yield different attention values for similar inputs and outputs. This however does not directly contradict the prediction assumption of faithfulness (Jacovi and Goldberg, 2020) as discussed by Wiegreffe and Pinter (2019). Closer to our work, the works Ivankay et al. (2021) and Sinha et al. (2021) are the first to prove that explanations in text classifiers are also susceptible to input changes in a very small local neighbourhood of the input. They introduce TEXTEXPLANATIONFOOLER (TEF) as a baseline to alter attributions and estimate local robustness of widely used attributions in text classification. However, the authors' definition of AR does not take semantic distances between original and adversarial samples into account. Thus their attack results in out-of-context and non-fluent adversarial samples, rendering such perturbations easier to detect, as it draws token substitution candidates from a separately trained custom synonym embedding.

3 Preliminaries

A text dataset $\mathbb{S}$ is comprised of N text samples $\boldsymbol{s}_i$, each containing a series of tokens w_j from a vocabulary $\mathbb{W}$ and true labels l_i drawn from the label set $\mathbb{L}$. A text classifier F is a function that maps each sample $\boldsymbol{s}_i$ to a label $y_i \in \mathbb{L}$. It consists of an embedding function E and a classifier function f. The embedding function $E : \mathbb{S} \to \mathbb{R}^{d \times p},\ E(\boldsymbol{s}) = \boldsymbol{X}$ maps the text samples $\boldsymbol{s}_i$ to a continuous embedding $\boldsymbol{X}$, while the classifier function $f : \mathbb{R}^{d \times p} \to \mathbb{R}^{|\mathbb{L}|},\ f(\boldsymbol{X}) = \boldsymbol{o}$ maps the embeddings to the output probabilities for each class.

An *attribution function* $A(\boldsymbol{s}, F, l) = \boldsymbol{a}$ assigns a real number to each token w_j in sample $\boldsymbol{s}$. This represents the tokens influence towards the classification outcome. A positive value represents a token that is deemed relevant *towards* the predicted label y, a negative value *against* it. We consider the attributions methods Saliency (S) (Simonyan et al., 2013), Integrated Gradients (IG) (Sundararajan et al., 2017) and Attention (A) (Bahdanau et al., 2014).

The *perplexity* (Keselj, 2009) of a text sample $\boldsymbol{s}$ with tokens w_j given a language model L measures how well the probability distribution given by L predicts sample $\boldsymbol{s}$, as defined in Equation (1):

$$PP(\boldsymbol{s}|L) = 2^{-\sum_{w_j \in \boldsymbol{s}} p(w_j|L,\boldsymbol{s}) \log p(w_j|L,\boldsymbol{s})} \quad (1)$$

where PP denotes the perplexity of the text sample $\boldsymbol{s}$ and $p(w_j|L, \boldsymbol{s})$ the probability of token w_j given L and $\boldsymbol{s}$. Low perplexity values indicate that the model L has well captured the true distribution of the text dataset $\mathbb{S}$.

Sentence encoders are embedding functions $E_s : \mathbb{S} \to \mathbb{R}^m,\ E_s(\boldsymbol{s}) = \boldsymbol{m}$ that assign a continuous embedding vector of dimension m to each text sample (Reimers and Gurevych, 2019). These embeddings are used to capture higher-level representations of the text samples or short paragraphs that can be used to train downstream tasks effectively.

4 Attribution Robustness

In this section, we introduce our new definition of attribution robustness (AR) in text classifiers. We describe our attribution and text distance measures. Furthermore, we introduce the optimization problem of estimating AR, our threat model as well as our novel estimator algorithm.

4.1 Attribution Robustness in Text

Most related work defines AR as the maximal attribution distance with a given locality constraint in the search space (Ivankay et al., 2021; Sinha et al., 2021). We argue that this is potentially problematic, as the perturbation size of the input is not taken into account. Two adversarial samples with similarly altered attributions might in fact strongly differ in terms of how well they maintain semantic similarity to the original sample (see e.g. 3$^{\text{rd}}$ example in Figure 1). This suggests that a proper measure of attribution robustness should ascribe

higher robustness to methods that are only vulnerable to larger perturbation while being impervious to imperceptible ones. Thus, we define attribution robustness for a given text sample $\boldsymbol{s}$ with true label l as functions of both resulting attribution distance and input perturbation size, written in Equation (2).

$$k(\boldsymbol{s}) = \max_{\tilde{\boldsymbol{s}} \in N(\boldsymbol{s})} \frac{d\big[A(\tilde{\boldsymbol{s}}, F, l),\ A(\boldsymbol{s}, F, l)\big]}{d_s(\tilde{\boldsymbol{s}}, \boldsymbol{s})} \tag{2}$$

with the constraint that the predicted classes of $\tilde{\boldsymbol{s}}$ and $\boldsymbol{s}$ are equal, written in Equation (3).

$$\arg\max_{i \in \{1 \ldots |\mathbb{L}|\}} F_i(\tilde{\boldsymbol{s}}) = \arg\max_{i \in \{1 \ldots |\mathbb{L}|\}} F_i(\boldsymbol{s}) \tag{3}$$

Here, d denotes the distance between attribution maps $A(\tilde{\boldsymbol{s}}, F, l)$ and $A(\boldsymbol{s}, F, l)$, F the sequence classifier with output probability F_i for class i, and d_s the distance of input text samples $\tilde{\boldsymbol{s}}$ and $\boldsymbol{s}$. $N(\boldsymbol{s})$ indicates a neighborhood of $\boldsymbol{s}$: $N(\boldsymbol{s}) = \tilde{\boldsymbol{s}} \mid d_s(\tilde{\boldsymbol{s}}, \boldsymbol{s}) < \varepsilon$ for a small ε. This definition is inspired by the Lipschitz continuity constant (Sohrab, 2003) and the robustness assumption of faithful explanations (Jacovi and Goldberg, 2020). The estimated attribution robustness of an attribution method A on a model F then becomes the expected per-sample $k(\boldsymbol{s})$ on dataset $\mathbb{S}$, see Equation (4).

$$k(A, F) = \mathbb{E}_{\boldsymbol{s} \in \mathbb{S}}\big[k(\boldsymbol{s})\big] \tag{4}$$

We call this k the estimated *Lipschitz attribution robustness (AR) constant*. The robustness of attribution method A on the model F is inversely proportional to $k(A, F)$, as high values correlate with large attribution distances and small input perturbations, which indicates low robustness.

4.2 Distances in Text Data

In order to compute the attribution robustness constants k from Equation (4), the distance measures in the numerator and denominator of Equation (2) need to be defined. In explainable AI, it is often argued that only the relative rank between input features or tokens is important when explaining the outcome of a classifier, or even only the top-k features. Users frequently focus on the features deemed most important to explain a decision and disregard the less important ones (Ivankay et al., 2020; Ghorbani et al., 2019; Dombrowski et al., 2019). Therefore, it is common practice (Ivankay et al., 2021; Sinha et al., 2021) to use correlation coefficients and top-k intersections as distance measures between attributions, as these tend to capture the human understanding of distance between explanations well. For this reason, we utilize the Pearson correlation coefficient (PCC) (Pearson, 1895) as attribution distance $d\big[A(\tilde{\boldsymbol{s}}, F, l),\ A(\boldsymbol{s}, F, l)\big] = 1 - \frac{1 + PCC\big[A(\tilde{\boldsymbol{s}}, F, l),\ A(\boldsymbol{s}, F, l)\big]}{2}$ of Equation (2).

Measuring distance between text inputs in the adversarial setting is not as straightforward as in the image domain, where L_p-norm induced distances are common. String distance metrics can only be used limitedly, as two words can have similar characters but entirely different meanings. For this reason, we propose the following set of measures to effectively capture the perturbation size in the denominator of Equation (2).

First, we utilize pretrained sentence encoders to measure the semantic textual similarity between the original and adversarial text samples. This can be computed by the cosine similarity between the sentence embeddings of the two text samples, see Equation (5).

$$d_{\mathrm{s}}(\tilde{\boldsymbol{s}}, \boldsymbol{s}) = 1 - \frac{s_{cos}[E_s(\tilde{\boldsymbol{s}}), E_s(\boldsymbol{s})] + 1}{2} \tag{5}$$

where d_{s} denotes the semantic distance between samples $\tilde{\boldsymbol{s}}$ and $\boldsymbol{s}$, s_{cos} the cosine similarity, and $E_s(\tilde{\boldsymbol{s}})$ and $E_s(\boldsymbol{s})$ the sentence embeddings of the two input samples. The semantic textual similarity provides a measure how close the two inputs are in their semantic meaning. To this end, the Universal Sentence Encoder (Cer et al., 2018) is widely-used in adversarial text setups (Sun et al., 2020; Ivankay et al., 2021). However, this architecture is not state-of-the-art on the STSBenchmark dataset (Cer et al., 2017), a benchmark used to evaluate semantic textual similarity. Therefore, we utilize a second sentence encoder architecture trained by the authors Wang et al. (2020), MiniLM. This model achieves close to state-of-the-art performance on the STS-Benchmark while maintaining a low computational cost.

Our second input distance is derived from the perplexity of original and adversarial inputs $\tilde{\boldsymbol{s}}$ and $\boldsymbol{s}$. We capture the relative increase of perplexity when perturbing the original sentence $\boldsymbol{s}$, given the pretrained GPT-2 language model (Radford et al., 2019) (Equation 6).

$$d_s(\tilde{\boldsymbol{s}}, \boldsymbol{s}) = \frac{PP(\tilde{\boldsymbol{s}}|L) - PP(\boldsymbol{s}|L)}{PP(\boldsymbol{s}|L) + \varepsilon} \tag{6}$$

where d_{s} denotes the distance between inputs $\tilde{\boldsymbol{s}}$ and

$\boldsymbol{s}$, PP the perplexity of the text sample given the GPT-2 language model L, ε a small constant.

Lastly, we capture the increase of grammatical errors in the input samples using the LanguageTool API [1]. As grammatical errors are easily perceived by the human observer, they significantly contribute to the perceptibility of adversarial perturbations (Ebrahimi et al., 2017).

4.3 Robustness Estimation

Given our AR definition in Equation (2), in order to estimate the true robustness of an attribution method for a given model, all possible input sequences $\tilde{s}$ within the neighbourhood N of $\boldsymbol{s}$ would have to be checked. This is a computationally intractable problem. Therefore we restrict the search space (i.e. the neighbourhood N) to sequences $\tilde{\boldsymbol{s}}$ that only contain token substitutions from the predefined vocabulary set $\mathbb{W}$. Moreover, we restrict the ratio of substituted tokens in the original sequence to ρ_{max}, considering only $|\mathbb{C}|$ number of possible substitutions for each token in $\boldsymbol{s}$. The number $|\mathbb{C}|$ is chosen to yield high attribution distance while keeping the computation cost low, detailed in Section 5. This way, we reduce the total perturbation set from $|\mathbb{W}|^{|\boldsymbol{s}|}$ to $|\mathbb{C}|^{|\boldsymbol{s}|\cdot\rho_{max}}$ samples. The adversarial sequence $\boldsymbol{s}_{\text{adv}}$ then becomes the perturbed sequence that maximizes $k(\boldsymbol{s})$ from Equation (2)

We estimate AR with our novel TRANSFORMEREXPLANATIONATTACK (TEA). TEA is a black-box attack, only having access to the model's prediction and the accompanying attributions, not the intermediate representations, architectural information or gradients. TEA consists of the following two steps.

Step 1: Word importance ranking. The first step extracts a priority ranking of tokens in the input text sample $\boldsymbol{s}$. For each word w_i in $\boldsymbol{s}$, TEA computes $I_{w_i} = d\big[A(\boldsymbol{s}_{w_i \to 0}, F, l),\ A(\boldsymbol{s}, F, l)\big]$, where $\boldsymbol{s}_{w_i \to 0}$ denotes the token w_i in $\boldsymbol{s}$ set to the zero embedding vector and d denotes the attribution distance measure in Equation (2), described in the previous subsection. The tokens in $\boldsymbol{s}$ are then sorted by descending values of I_{w_i}. Thus, we estimate words that are *likely* to result in large attribution distances and prioritize those for substitutions towards building explanation attacks.

Step 2: Candidate selection and substitution. The second step of TEA substitutes each highest ranked token in $\boldsymbol{s}$, computed in **Step 1**, with a token from a candidate set $\mathbb{C}$, in descending importance order. Each highest ranked token has its separate candidate set $\mathbb{C}$. TEA extracts these candidate sets by masking them and querying a transformer-based masked language model (MLM). In order to keep the computational costs low, we utilize the DistilBERT pretrained masked language model (Sanh et al., 2019), a BERT-MLM with significantly fewer parameters and more computationally efficient. Also, at most $n = |\boldsymbol{s}| \cdot \rho_{max}$ words are substituted.

In order to further reduce computational cost, TEA uses batch masking. Thus, instead of masking each token separately and querying the MLM for candidates, the first $n_b = |\boldsymbol{s}| \cdot \rho_b$ most important tokens are masked at once and the language model is queried for candidates for all of these masked tokens. Here, n_b denotes the number, ρ_b the ratio of tokens in $\boldsymbol{s}$ to be masked at once. For instance,

Algorithm 1 `TransformerExplanationAttack`

Input: Input sentence $\boldsymbol{s}$ with predicted class l, classifier F, attribution A, attribution distance d, DistilBERT-MLM L, number of candidates N, maximum perturbation ratio ρ_{max}, batch masking ratio ρ_b

Output: Adversarial sentence $\boldsymbol{s}_{\text{adv}}$

$\boldsymbol{s}_{\text{adv}} \leftarrow \boldsymbol{s}$, $d_{max} \leftarrow 0$, $r \leftarrow 0$
for $w_i \in \boldsymbol{s}$ **do**
  $I_{w_i} = d\big[A(\boldsymbol{s}_{w_i \to 0}, F, l),\ A(\boldsymbol{s}, F, l)\big]$
$\boldsymbol{s}_B \leftarrow \langle \boldsymbol{s}_{1...b}, \boldsymbol{s}_{b+1...2b}, ..., \boldsymbol{s}_{|\boldsymbol{s}|-b+1...|\boldsymbol{s}|} \rangle$ with $I_{w_{b-1}} \geq I_{w_b}\ \forall j \in \{2, ..., |\boldsymbol{s}_B|\}$ and $\forall b \in \{1, .., |\boldsymbol{s}_j|\}$
for $\boldsymbol{s}_b \in \boldsymbol{s}_B$ **do**
  $\mathbb{C}_{\mathbf{b}} \leftarrow L(\boldsymbol{s}_{b \to [MASK]}, \boldsymbol{s}_{\text{adv}})$
  for $w_j \in \boldsymbol{s}_b$ **do**
    if $w_j \in \mathbb{S}_{\texttt{Stop words}}$ **then**
      continue
    for $c_k \in \mathbb{C}_j$ **do**
      $\tilde{\boldsymbol{s}}_{w_j \to c_k} \leftarrow$ Replace w_j in $\boldsymbol{s}_{\text{adv}}$ with c_k
      if $\underset{i \in \{1:|\mathbb{L}|\}}{\arg\max} F(\tilde{\boldsymbol{s}}_{w_j \to c_k}) \neq l$ **then**
        continue
      $\tilde{d} = d\big[A(\tilde{\boldsymbol{s}}_{w_i \to c_k}, F, l), A(\boldsymbol{s}, F, l)\big]$
      if $\tilde{d} > d_{max}$ **then**
        $\boldsymbol{s}_{\text{adv}} \leftarrow \tilde{\boldsymbol{s}}_{w_i \to c_k}$
        $d_{max} \leftarrow \tilde{d}$
        $r \leftarrow r + 1$
    if $\rho = \frac{r}{|\boldsymbol{s}|} + 1 > \rho_{max}$ **then**
      break

[1] https://languagetool.org

during AR estimation of a 100 word text sample, given $\rho_{max} = 0.15$ and $\rho_b = 0.05$, the MLM is queried only $(100 \cdot 0.15)/(100 \cdot 0.05) = 3$ times with batch masking instead of $100 \cdot 0.15 = 15$ times without it. We have compared the runtime of TEA using non-distilled (Devlin et al., 2018) and distilled (Sanh et al., 2019) BERT MLMs, with and without batch masking, and found considerable performance increase with batch masking and distillation. The results are reported in Section 5.

5 Experiments

In this section, we present our AR estimation experiments. Specifically, we describe the evaluation setup and results with our novel robustness definition. We show that TEA consistently outperforms our direct state-of-the-art competitor, TEXTEXPLANATIONFOOLER (TEF) in terms of the Lipschitz attribution robustness constant *k* described in Section 4. Thus, we convey that TEA extracts smoother adversarial samples that are able to alter attributions more significantly than TEF. Finally, we compare the runtime of TEA to TEF and show that TEA achieves comparable runtimes, while still outperforming TEF in the previously mentioned aspects.

5.1 Setup

We evaluate the robustness constant *k* estimated by TEA on the AG's News (Zhang et al., 2015), MR Movie Reviews (Zhang et al., 2015), IMDB Review (Maas et al., 2011), Yelp (Asghar, 2016) and the Fake News datasets [2]. We train a CNN, an LSTM, an LSTM with an attention layer (LSTMAtt), a finetuned BERT (Devlin et al., 2018), RoBERTA (Liu et al., 2019) and XLNet (Yang et al., 2019) classifier for each dataset. A detailed description of these can be found in the appendix. We estimate the robustness of the Saliency (S), Integrated Gradients (IG) and Attention (A) attribution methods. The CNN and LSTM architectures are only used in combination with S and IG, the remaining LSTMAtt, BERT, RoBERTA and XLNet are used with all three attribution methods. Thus, we evaluate $2 \cdot 2 + 4 \cdot 3 = 16$ combinations of models and attributions for each dataset.

We vary the ρ_{max} parameter of TEA between 0.01 and 0.4. A value of ρ_{max} does not necessarily lead to the actual perturbed ratio of tokens ρ to be $\rho = \rho_{max}$, due to the prediction constraint. We set the batch masking size $\rho_b = \min(\rho_{max}, 0.15)$, as the MLM we use was trained by masking approximately 15% of the tokens (Sanh et al., 2019). We set $|\mathbb{C}| = 15$ for each run. Larger values do not tend to result in better estimation in terms of k, but to significantly higher attack runtimes. Moreover, this makes our experiments comparable to TEF (Ivankay et al., 2021).

Our attack and experiments are implemented in PyTorch (Paszke et al., 2019), utilizing the Hugging Face Transformer library (Wolf et al., 2020), Captum (Kokhlikyan et al., 2020) and SpaCy (Honnibal et al., 2020). We run each experiment on an NVIDIA A100 GPU with three different seeds and report the average results.

5.2 Results

We report the following metrics as functions of the true perturbed ratio ρ. The average PCC values of original and adversarial attribution maps indicate the amount of change in explanations. Lower values correspond to larger attribution changes. The input distance between text samples is captured by the semantic textual similarity values of the original and adversarial samples, measured by the cosine similarity between the corresponding USE (Cer et al., 2018) and MiniLM (Wang et al., 2020) sentence embeddings (STS_{USE} and STS_{MiniLM}), as well as the relative perplexity increase (Δ_{PP}). Moreover, the average increase in number of grammatical errors (GE) after perturbation is also reported. Using these values, we report the estimated Lipschitz robustness constants k_{USE}, k_{MiniLM} and k_{PP}, according to Equation (4). In each of these, the scaled PCC is used as attribution distance. We compare these metrics for both our novel TEA algorithm and the direct competitor method TEF (Ivankay et al., 2021). Figure 2 reports these metrics as a function of the true perturbed token ratio ρ. The continuous lines contain the reported metrics for our TEA attack, the dashed lines for the competitor TEF. The figure shows that TEA perturbations are able to alter explanations more (lower average PCC values), and they do so with adversarial samples equally or more semantically similar to the original inputs than TEF (higher average STS, lower average PP and GE values). Moreover, the perplexity increase is consistently lower for TEA perturbations, leading to more fluent adversarial samples. This is well-captured by resulting robustness constants k, which are consistently higher for TEA than TEF, showing both

[2] https://www.kaggle.com/c/fake-news/data

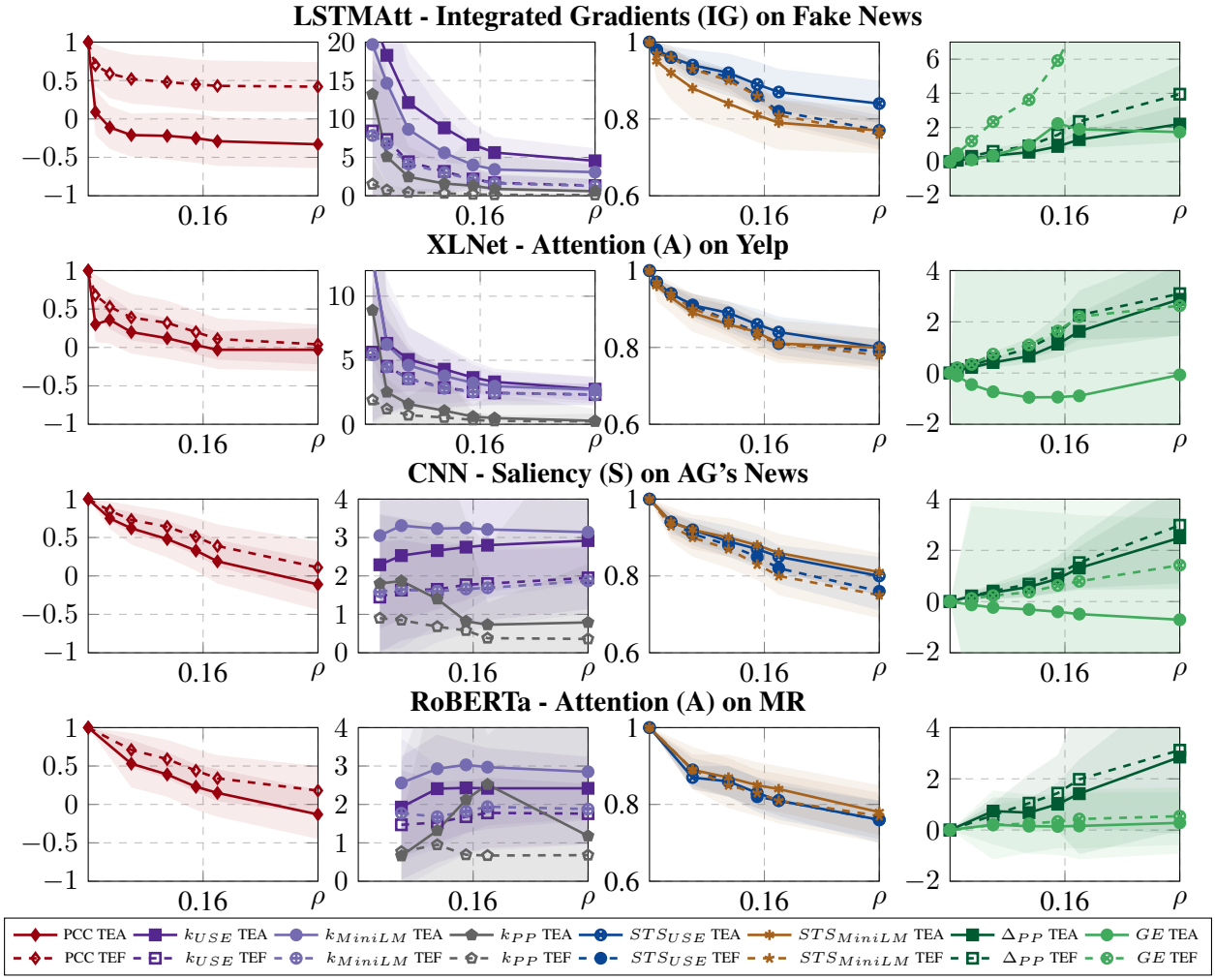


Figure 2: AR metrics as functions of the ratio of perturbed tokens ρ. We plot the mean and standard deviation of the Pearson correlations (PCC) between original and adversarial attributions, semantic similarities (STS), relative perplexity increase (Δ_{PP}), increase of number of grammatical errors (GE) in original and adversarial text inputs and the estimated AR robustness constants (k). We compare these values for our novel TRANSFORMEREXPLANATIONATTACK (TEA - continuous lines) and the current state-of-the-art TEXTEXPLANATIONFOOLER (TEF - dashed lines). We observe consistent improvement of robustness estimation with TEA compared to TEF, reflected in higher resulting k-values. This is attributed to both lower PCC values, higher semantic similarities of perturbed sentences to the original ones and lower adversarial perplexity of TEA perturbations.

that our AR definition of Equation (2) is a suitable indicator for AR in text classifiers, and that TEA estimates this robustness better than the state-of-the-art TEF attack. The rest of the results is reported in the appendix.

In order to quantify the overall performance of TEA over the whole operation interval of ρ, we compute the area under the estimated $k - \rho$ curves (2^{nd} column in Figure 2). These are calculated as the integral $\text{AUC}_k = \int_\rho k(A, F)d\rho$. High AUC_k values correspond to high k-values, thus low overall robustness of attributions. We then compare the resulting AUC_k estimated with our TEA algorithm to the competitor method TEF. Figure 3 shows the relative increase of AUC when estimating with TEA rather than TEF, for each of the 16 combinations of models and attribution methods for a given dataset. For instance, a value of 0.5 indicates a relative increase of 50% in estimated AUC_k, i.e. if TEF results in $\text{AUC}_k = 1.0$, TEA yields $\text{AUC}_k = 1.5$. We plot the AUC_k increase estimated with the semantic textual similarities from USE (AUC_k^{USE}), MiniLM (AUC_k^{MiniLM}) and with the relative perplexity increase (AUC_k^{PP}) in the denominator of k. The attribution distance in the numerator of k is set to the PCC described in Section (4). We observe an increase in AUC_k of $0.3 - 0.5$ in case of USE and TSE, and $0.5 - 1.5$ in

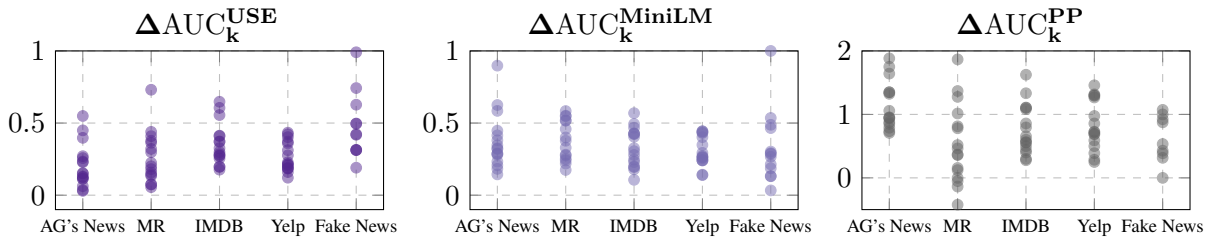


Figure 3: Relative increase Δ of AUC_k when estimating the robustness constants k (Equation 4) with TEA compared to TEF. Each point corresponds to one of the 16 combinations of model and attribution method, on the indicated dataset. The k-values are estimated with the PCC as attribution similarity, varying the input distance measures d_s as described in Section 4.2. We observe a relative increase of $0.3 - 1.5$ for almost all models, attribution maps and datasets evaluated on. This shows that TEA consistently provides better perturbations that alter attributions more while being more fluent and semantically similar to the unperturbed input.

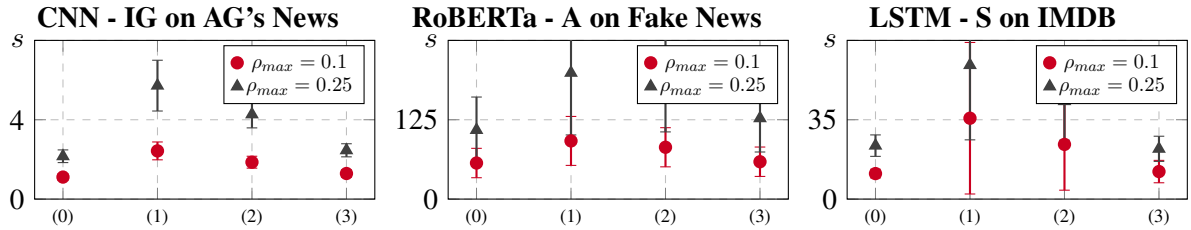


Figure 4: Per-sample runtime (s) of our AR estimator algorithm versions. TEA (3), with a distilled MLM and batch masking, achieves comparably fast estimation as TEF (0), while TEA with a non-distilled BERT MLM (1) is the slowest estimator, with a relative increase in runtime of approx. 1.5-2.5 compared to TEF. Distillation of the MLM (2) improves the runtime by around 25-35% compared to (1).

case of PP for most models, attribution maps and datasets. This further shows that TEA consistently yields higher robustness constants k than TEF, providing better perturbations that alter attributions more while being more fluent and less perceptible.

Querying transformer-based masked language models (MLMs) is computationally expensive. Naively substituting the synonym extraction from TEF with an MLM-based candidate extraction results in a significant increase in estimation time. Therefore, we use the methods described in Section 4 to achieve comparable estimation time in our TEA algorithm and TEF. Figure 4 contains the per-sample attack time for TEF (0), TEA with the non-distilled BERT MLM (1), TEA with DistilBERT MLM (2) and our final TEA algorithm with DistilBERT MLM and batch masking (3), for $\rho_{max} \in \{0.1, 0.25\}$. We observe that (1) results in a significant increase in mean estimation time by a factor of around 2 compared to (0) on both a smaller, medium and a larger datasets. Using (2) for estimating AR decreases the runtime by a large margin compared to (1). Finally, when applying both a distilled MLM and batch masking - TEA (3), the per-sample attack time is comparable to the baseline TEF, while maintaining better AR estimation performance.

6 Conclusion

In this work, we introduced a novel definition of attribution robustness in text classifiers, derived from the notion of Lipschitz-continuity. Crucially, our definition incorporates the size of the perturbations, which contributes significantly to perceptibility. To this end, we introduce semantic textual similarity measures, the relative perplexity increase and the number of grammatical errors as ways to effectively quantify perturbation size in text. Moreover, we introduced TRANSFORMEREXPLANATIONATTACK, a novel state-of-the-art attack method that results in a tighter estimator for attribution robustness in text classification problems. It is a black box estimator that utilizes a distilled MLM with batch masking to extract good adversarial perturbations with small computational overhead. Finally, we showed that TEA outperforms current attack methods by altering explanations more significantly using less perceptible perturbations.

In future work, we plan to examine the robustness of a wider variety of attributions, develop methods that improve explanation robustness and adapt the novel techniques to real-life scenarios.

References

Nabiha Asghar. 2016. Yelp dataset challenge: Review rating prediction. *arXiv preprint arXiv:1605.05362*.

Dzmitry Bahdanau, Kyunghyun Cho, and Yoshua Bengio. 2014. Neural machine translation by jointly learning to align and translate. *arXiv preprint arXiv:1409.0473*.

Daniel Cer, Mona Diab, Eneko Agirre, Inigo Lopez-Gazpio, and Lucia Specia. 2017. Semeval-2017 task 1: Semantic textual similarity-multilingual and cross-lingual focused evaluation. *arXiv preprint arXiv:1708.00055*.

Daniel Cer, Yinfei Yang, Sheng-yi Kong, Nan Hua, Nicole Limtiaco, Rhomni St John, Noah Constant, Mario Guajardo-Céspedes, Steve Yuan, Chris Tar, et al. 2018. Universal sentence encoder. *arXiv preprint arXiv:1803.11175*.

Jiefeng Chen, Xi Wu, Vaibhav Rastogi, Yingyu Liang, and Somesh Jha. 2019. Robust Attribution Regularization. In *Advances in Neural Information Processing Systems*, pages 14300–14310.

Jacob Devlin, Ming-Wei Chang, Kenton Lee, and Kristina Toutanova. 2018. Bert: Pre-training of deep bidirectional transformers for language understanding. *arXiv preprint arXiv:1810.04805*.

Ann-Kathrin Dombrowski, Maximillian Alber, Christopher Anders, Marcel Ackermann, Klaus-Robert Müller, and Pan Kessel. 2019. Explanations can be manipulated and geometry is to blame. In *Advances in Neural Information Processing Systems*, pages 13589–13600.

Javid Ebrahimi, Anyi Rao, Daniel Lowd, and Dejing Dou. 2017. Hotflip: White-box adversarial examples for text classification. *arXiv preprint arXiv:1712.06751*.

Amirata Ghorbani, Abubakar Abid, and James Zou. 2019. Interpretation of neural networks is fragile. In *Proceedings of the AAAI Conference on Artificial Intelligence*, volume 33, pages 3681–3688.

Ivan Girardi, Pengfei Ji, An-phi Nguyen, Nora Hollenstein, Adam Ivankay, Lorenz Kuhn, Chiara Marchiori, and Ce Zhang. 2018. Patient risk assessment and warning symptom detection using deep attention-based neural networks. *arXiv preprint arXiv:1809.10804*.

Matthew Honnibal, Ines Montani, Sofie Van Landeghem, and Adriane Boyd. 2020. spaCy: Industrial-strength Natural Language Processing in Python.

Adam Ivankay, Ivan Girardi, Chiara Marchiori, and Pascal Frossard. 2020. Far: A general framework for attributional robustness. *arXiv preprint arXiv:2010.07393*.

Adam Ivankay, Ivan Girardi, Chiara Marchiori, and Pascal Frossard. 2021. Fooling explanations in text classifiers. In *International Conference on Learning Representations*.

Alon Jacovi and Yoav Goldberg. 2020. Towards faithfully interpretable nlp systems: How should we define and evaluate faithfulness? *arXiv preprint arXiv:2004.03685*.

Sarthak Jain and Byron C Wallace. 2019. Attention is not explanation. *arXiv preprint arXiv:1902.10186*.

Vlado Keselj. 2009. Speech and language processing daniel jurafsky and james h. martin (stanford university and university of colorado at boulder) pearson prentice hall, 2009, xxxi+ 988 pp; hardbound, isbn 978-0-13-187321-6, $115.00.

Narine Kokhlikyan, Vivek Miglani, Miguel Martin, Edward Wang, Bilal Alsallakh, Jonathan Reynolds, Alexander Melnikov, Natalia Kliushkina, Carlos Araya, Siqi Yan, et al. 2020. Captum: A unified and generic model interpretability library for pytorch. *arXiv preprint arXiv:2009.07896*.

Yinhan Liu, Myle Ott, Naman Goyal, Jingfei Du, Mandar Joshi, Danqi Chen, Omer Levy, Mike Lewis, Luke Zettlemoyer, and Veselin Stoyanov. 2019. Roberta: A robustly optimized bert pretraining approach. *arXiv preprint arXiv:1907.11692*.

Andrew Maas, Raymond E Daly, Peter T Pham, Dan Huang, Andrew Y Ng, and Christopher Potts. 2011. Learning word vectors for sentiment analysis. In *Proceedings of the 49th annual meeting of the association for computational linguistics: Human language technologies*, pages 142–150.

Seyed-Mohsen Moosavi-Dezfooli, Alhussein Fawzi, Jonathan Uesato, and Pascal Frossard. 2019. Robustness via curvature regularization, and vice versa. In *Proceedings of the IEEE/CVF Conference on Computer Vision and Pattern Recognition*, pages 9078–9086.

Adam Paszke, Sam Gross, Francisco Massa, Adam Lerer, James Bradbury, Gregory Chanan, Trevor Killeen, Zeming Lin, Natalia Gimelshein, Luca Antiga, et al. 2019. Pytorch: An imperative style, high-performance deep learning library. In *Advances in Neural Information Processing Systems*, pages 8026–8037.

Karl Pearson. 1895. Notes on regression and inheritance in the case of two parents. *Proceedings of the Royal Society of London*, 58(347-352):240–242.

Alec Radford, Jeffrey Wu, Rewon Child, David Luan, Dario Amodei, Ilya Sutskever, et al. 2019. Language models are unsupervised multitask learners. *OpenAI blog*, 1(8):9.

Nils Reimers and Iryna Gurevych. 2019. Sentence-bert: Sentence embeddings using siamese bert-networks. *arXiv preprint arXiv:1908.10084*.

Mattia Rigotti, Christoph Miksovic, Ioana Giurgiu, Thomas Gschwind, and Paolo Scotton. 2022. Attention-based interpretability with concept transformers. In *International Conference on Learning Representations*.

Victor Sanh, Lysandre Debut, Julien Chaumond, and Thomas Wolf. 2019. Distilbert, a distilled version of bert: smaller, faster, cheaper and lighter. *arXiv preprint arXiv:1910.01108*.

Avanti Shrikumar, Peyton Greenside, and Anshul Kundaje. 2017. Learning important features through propagating activation differences. *arXiv preprint arXiv:1704.02685*.

Karen Simonyan, Andrea Vedaldi, and Andrew Zisserman. 2013. Deep inside convolutional networks: Visualising image classification models and saliency maps. *arXiv preprint arXiv:1312.6034*.

Sanchit Sinha, Hanjie Chen, Arshdeep Sekhon, Yangfeng Ji, and Yanjun Qi. 2021. Perturbing inputs for fragile interpretations in deep natural language processing. *arXiv preprint arXiv:2108.04990*.

Houshang H Sohrab. 2003. *Basic real analysis*, volume 231. Springer.

Lichao Sun, Kazuma Hashimoto, Wenpeng Yin, Akari Asai, Jia Li, Philip Yu, and Caiming Xiong. 2020. Adv-bert: Bert is not robust on misspellings! generating nature adversarial samples on bert. *arXiv preprint arXiv:2003.04985*.

Mukund Sundararajan, Ankur Taly, and Qiqi Yan. 2017. Axiomatic attribution for deep networks. In *Proceedings of the 34th International Conference on Machine Learning*, volume 70, pages 3319–3328.

Wenhui Wang, Furu Wei, Li Dong, Hangbo Bao, Nan Yang, and Ming Zhou. 2020. Minilm: Deep self-attention distillation for task-agnostic compression of pre-trained transformers. *Advances in Neural Information Processing Systems*, 33:5776–5788.

Sarah Wiegreffe and Yuval Pinter. 2019. Attention is not not explanation. *arXiv preprint arXiv:1908.04626*.

Thomas Wolf, Lysandre Debut, Victor Sanh, Julien Chaumond, Clement Delangue, Anthony Moi, Pierric Cistac, Tim Rault, Rémi Louf, Morgan Funtowicz, Joe Davison, Sam Shleifer, Patrick von Platen, Clara Ma, Yacine Jernite, Julien Plu, Canwen Xu, Teven Le Scao, Sylvain Gugger, Mariama Drame, Quentin Lhoest, and Alexander M. Rush. 2020. Transformers: State-of-the-art natural language processing. In *Proceedings of the 2020 Conference on Empirical Methods in Natural Language Processing: System Demonstrations*, pages 38–45, Online. Association for Computational Linguistics.

Zhilin Yang, Zihang Dai, Yiming Yang, Jaime Carbonell, Russ R Salakhutdinov, and Quoc V Le. 2019. Xlnet: Generalized autoregressive pretraining for language understanding. *Advances in neural information processing systems*, 32.

Xiang Zhang, Junbo Jake Zhao, and Yann LeCun. 2015. Character-level convolutional networks for text classification. In *NIPS*.

A Appendix

A.1 Datasets

We estimate the robustness of our attribution methods and models on five publicly available datasets. These are AG's News, MR movie review, IMDB movie review, Yelp and Fake News, all of which are English language. AG's News consists of 127552 news article samples, categorized into the classes World, News, Business and Sci/Tech. We use the concatenation of title and text of the samples to feed into our text classifiers, stripping any sample that is longer than 64 tokens. The MR movie review dataset contains 10592 short samples of positive or negative movie reviews. We only use the first 32 tokens in each sample as input to the classifiers. IMDB movie review is a dataset consisting of 49952 positive and negative movie reviews, with a maximum token length of 256. Yelp categorizes 700000 reviews of several topics into 5 classes, each representing a rating from 1 to 5. We strip the samples to a maximum length of 256. Fake News is a collection of 20080 news samples, each categorized into reliable or unreliable. These are rather long articles, thus we use a maximum sequence length of 512 for this dataset.

We apply basic preprocessing to all samples in each dataset, which includes converting them to lowercase, removing any special characters not in the English alphabet and emojis. We use 60% of the samples for training the classifier models, 20% for validation and 20% for testing and estimating the robustness of attribution methods.

DATASET	CNN	LSTM	LSTMATT	BERT	ROBERTA	XLNET
AG'S NEWS	89.7%	90.8%	91.4%	94.2%	94.0%	93.8%
MR	73.0%	76.4%	78.0%	82.2%	87.7%	86.3%
IMDB	82.0%	87.2%	87.3%	89.4%	93.3%	93.7%
YELP	49.0%	54.8%	60.0%	62.6%	67.6%	-
FAKE NEWS	98.9%	99.6%	99.6%	99.8%	100.0%	100.0%

Table 1: Classifier accuracies

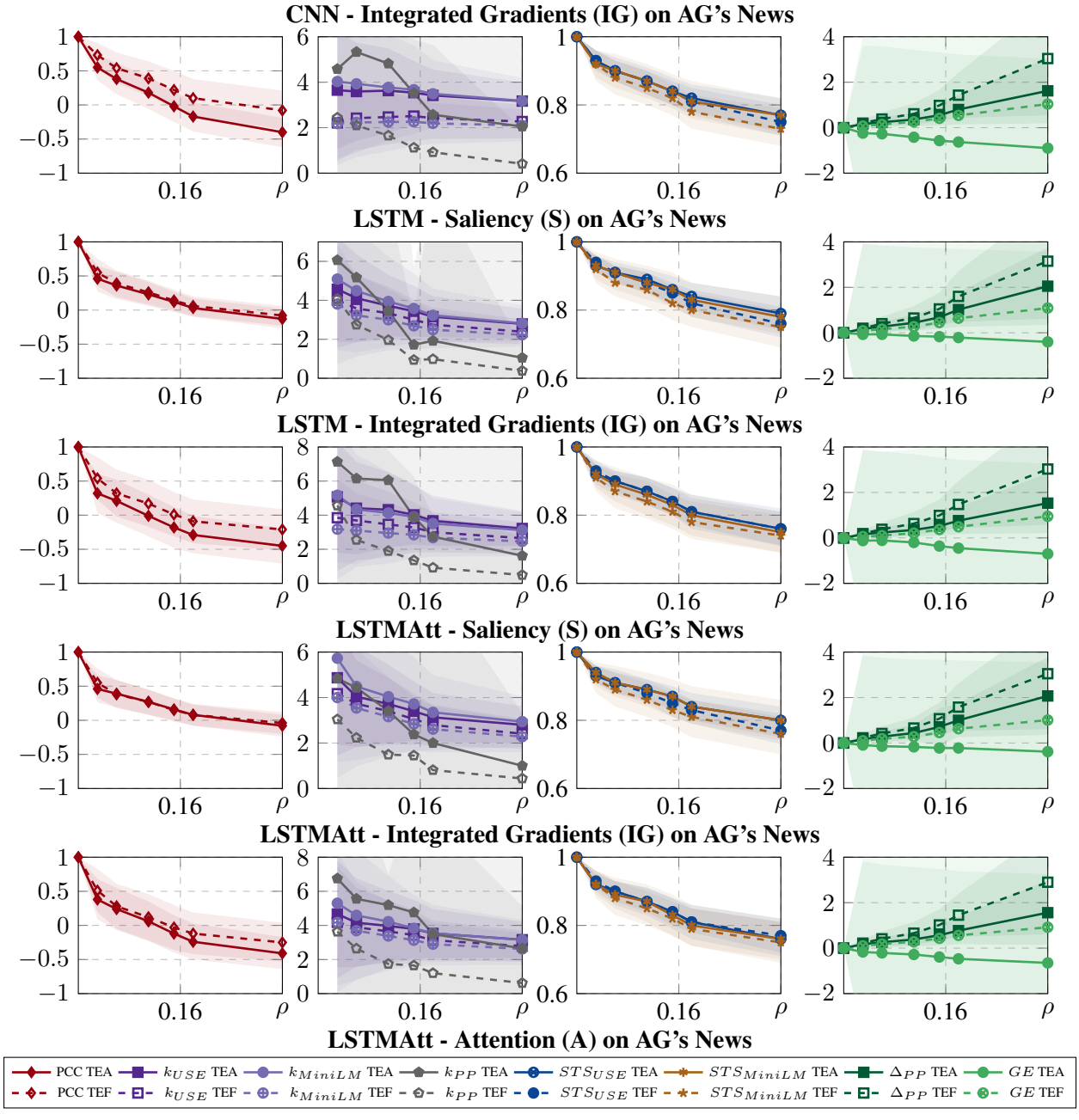
A.2 Models

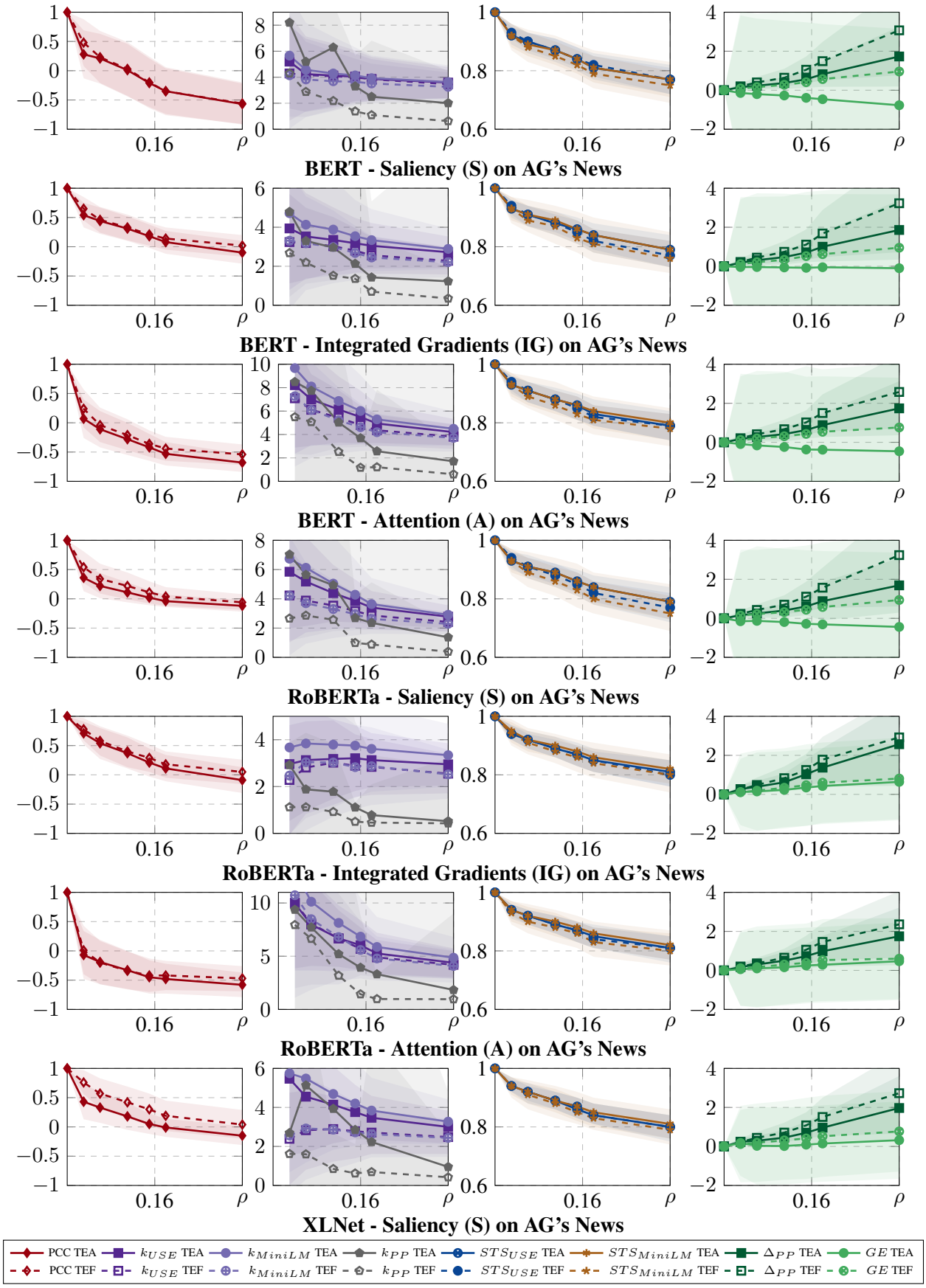
		AG's News	MR	IMDB	Yelp	Fake News
CNN	Input shape	(64, 300)	(32,300)	(256, 300)	(256, 300)	(512, 300)
	Num. classes	4	2	2	5	2
	Filter sizes	[3, 5, 7]	[3, 5]	[3, 5, 7]	[3, 5, 7]	[3, 5, 7]
	Feature sizes	[8, 8, 8]	[8, 8]	[16, 16, 16]	[128, 128, 128]	[32, 32, 32]
	Pooling sizes	[2, 2, 2]	[2, 2]	[2, 2, 2]	[2, 2, 2]	[2, 2, 2]
	Lin. layer dim.	8	8	16	64	32
	Num. params	67748	27946	567458	16428293	4091714
LSTM	Input shape	(64, 300)	(32,300)	(256, 300)	(256, 300)	(512, 300)
	Num. classes	4	2	2	5	2
	Hidden dim.	8	8	16	256	16
	Num. layers	1	1	2	2	1
	Pooling sizes	2	2	1	2	2
	Lin. layer dim.	8	8	16	32	16
	Num. params	10988	10458	18162	2146693	85986
LSTMAtt	Input shape	(64, 300)	(32,300)	(256, 300)	(256, 300)	(512, 300)
	Num. classes	4	2	2	5	2
	Hidden dim.	8	8	16	256	16
	Num. layers	4	1	2	2	1
	Lin. layer dim.	8	8	16	32	16
	Num. params	25004	19994	47666	2752901	41826
BERT	Input shape	(64,)	(32,)	(256,)	(256,)	(512,)
	Num. classes	4	2	2	5	2
	Model ID	bert-base-uncased	bert-base-uncased	bert-base-uncased	bert-base-uncased	bert-base-uncased
	Num. params	109485316	109483778	109483778	109486085	109483778
RoBERTa	Input shape	(64,)	(32,)	(256,)	(256,)	(512,)
	Num. classes	4	2	2	5	2
	Model ID	roberta-base	roberta-base	roberta-base	roberta-base	roberta-base
	Num. params	124648708	124647170	124647170	124649477	124647170
XLNet	Input shape	(64,)	(32,)	(256,)	(256,)	(512,)
	Num. classes	4	2	2	5	2
	Model ID	xlnet-base-cased	xlnet-base-cased	xlnet-base-cased	xlnet-base-cased	xlnet-base-cased
	Num. params	117312004	117310466	117310466	117312773	117310466

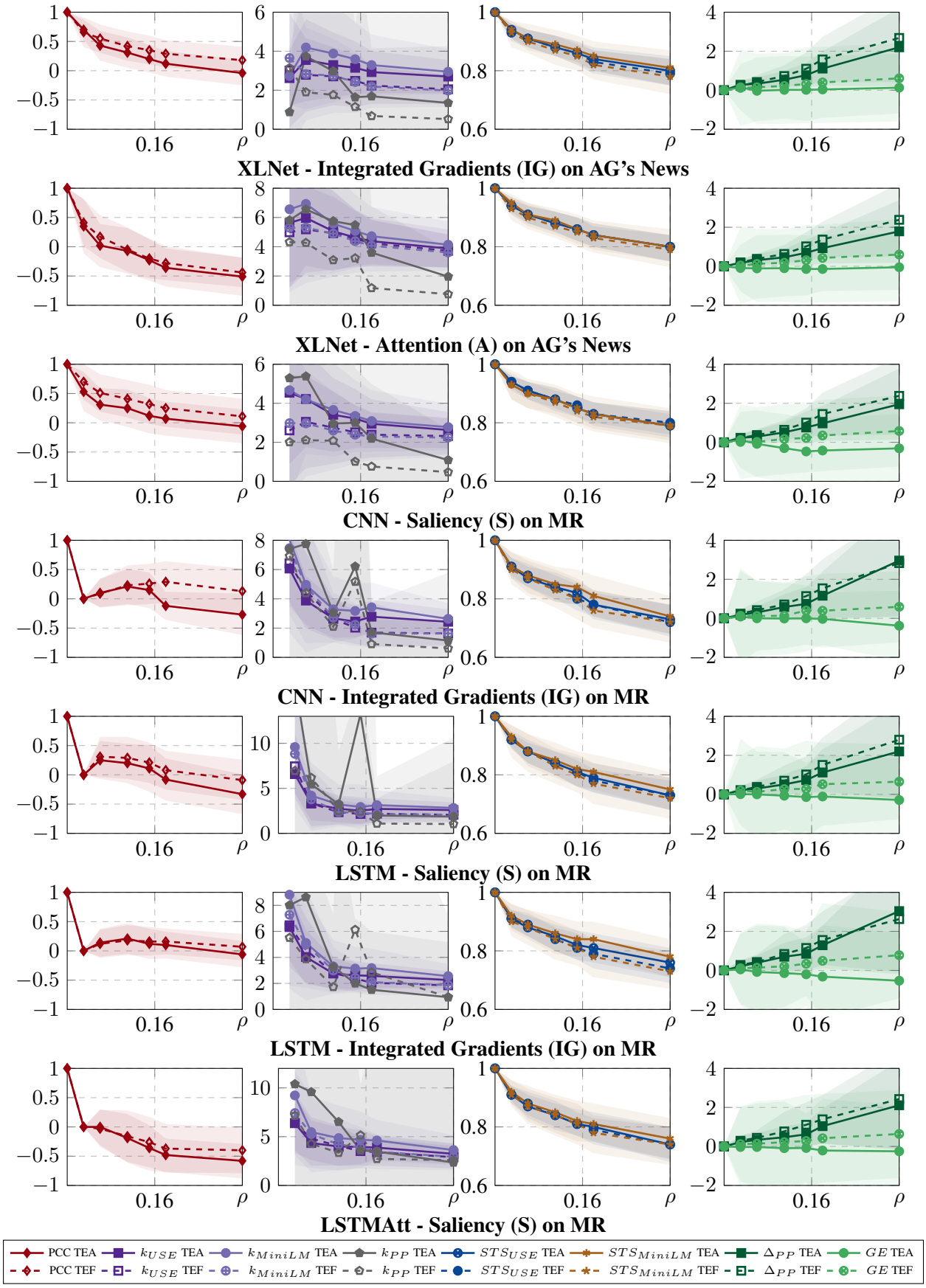
Table 2: Model specifications

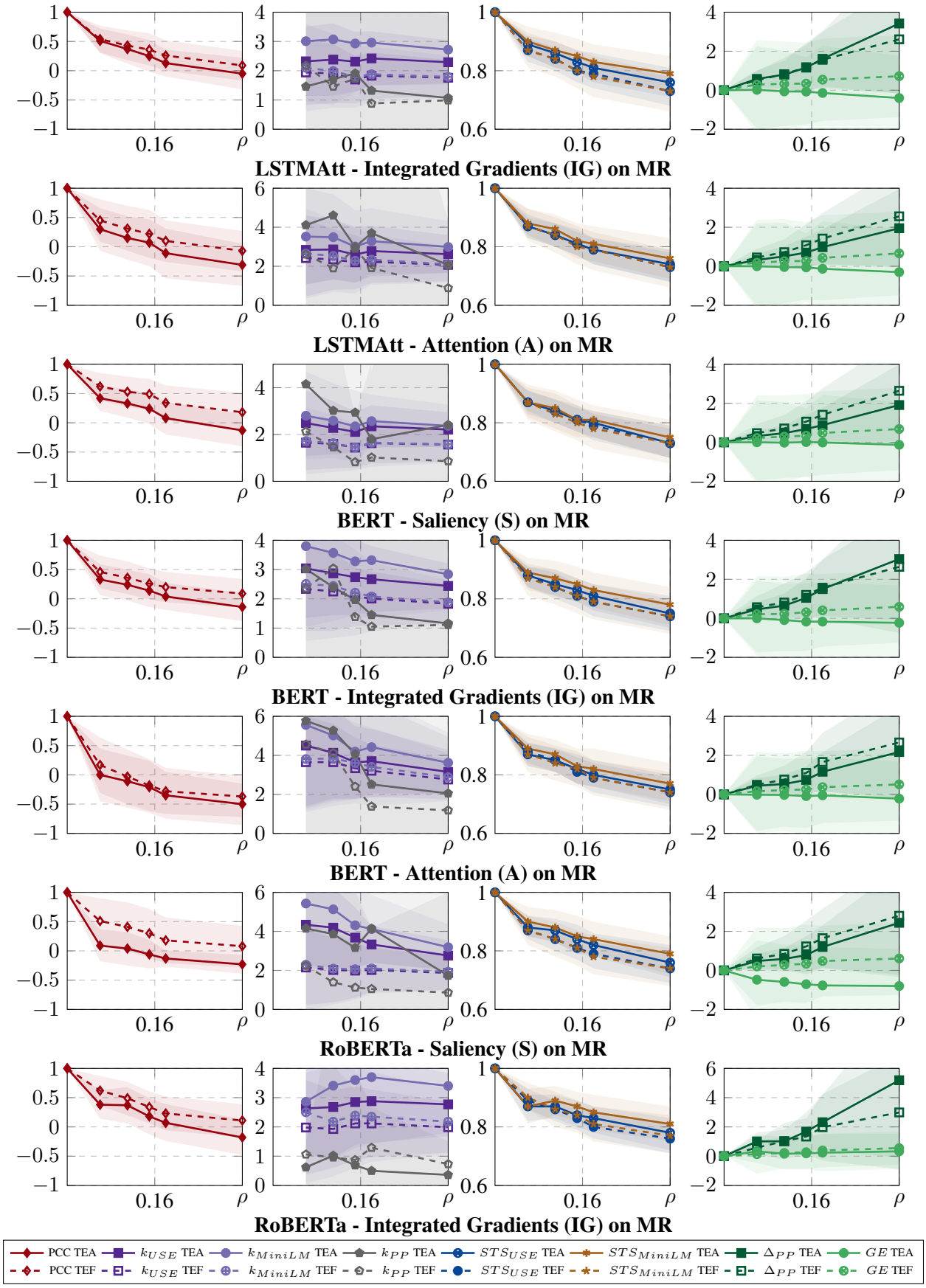
As described in the main paper, we train six classification architectures for each dataset, three DNN-based architectures, which are a CNN, an LSTM, an LSTM with an attention layer (LSTMAtt), as well as three transformer-based architectures, which are a finetuned BERT, RoBERTa and XLNet. The CNN, LSTM and LSTMAtt architectures use the 6B-300-dimensional Glove word embeddings, while the transformer-based architectures use the pretrained Huggingface embeddings of the respective base-uncased versions. During training, the embeddings are not trained, only the model parameters. The DNN-based classifiers each contain a linear layer on top of their feature extractors and use the built-in SpaCy English tokenizer, the transformers directly map the feature outputs to the output logits with a fully-connected layer and utilize the Huggingface preptrained tokenizers for each architecture respectively. Table 2 contains the model specifications. We train each model with a standard learning rate of 0.001, using the cross-entropy loss and early stopping. We utilize NVIDIA A100 GPUs to speed up training and AR estimation. The resulting accuracies of the models can be found in Table 1.

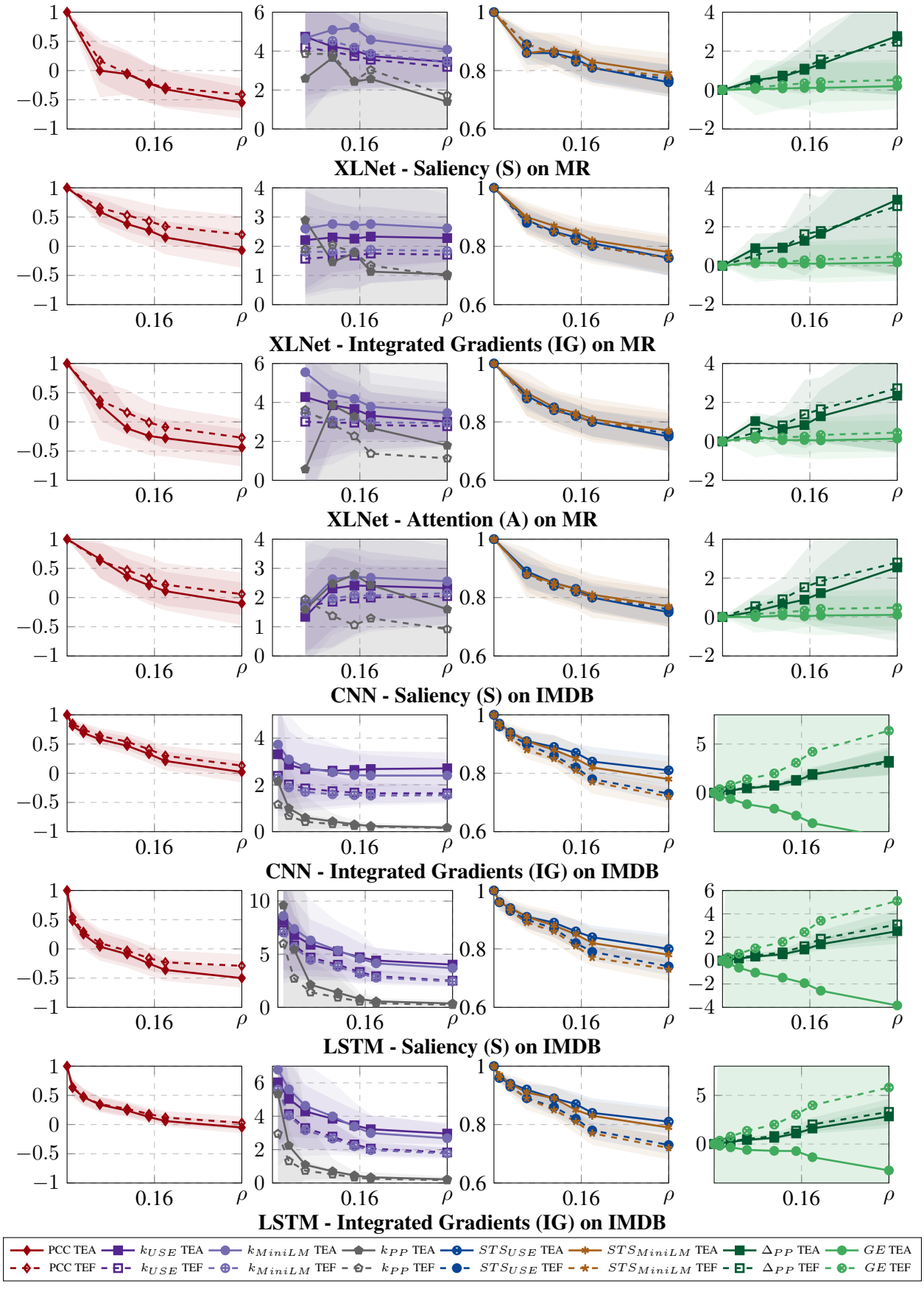
A.3 Additional AR results

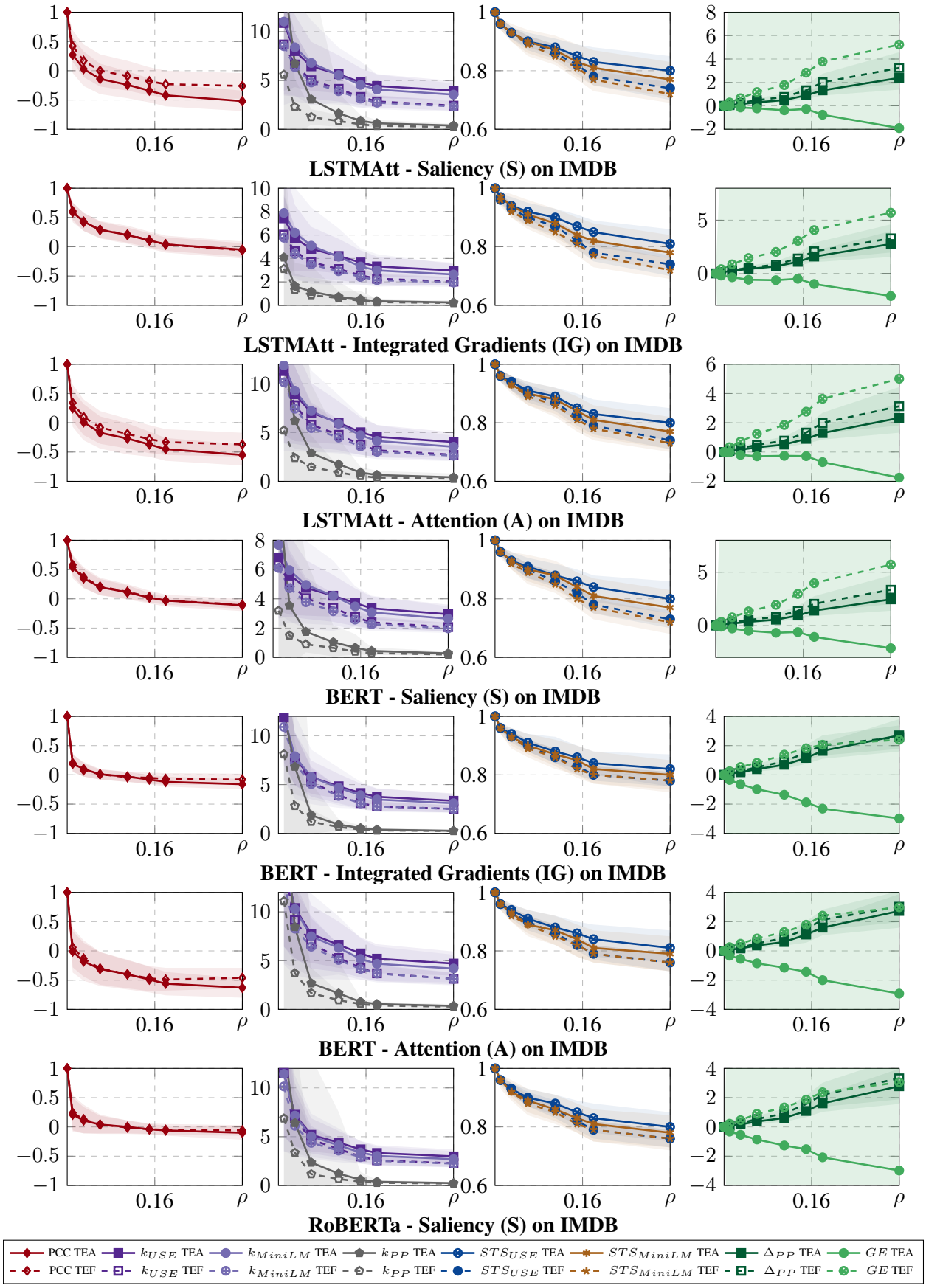


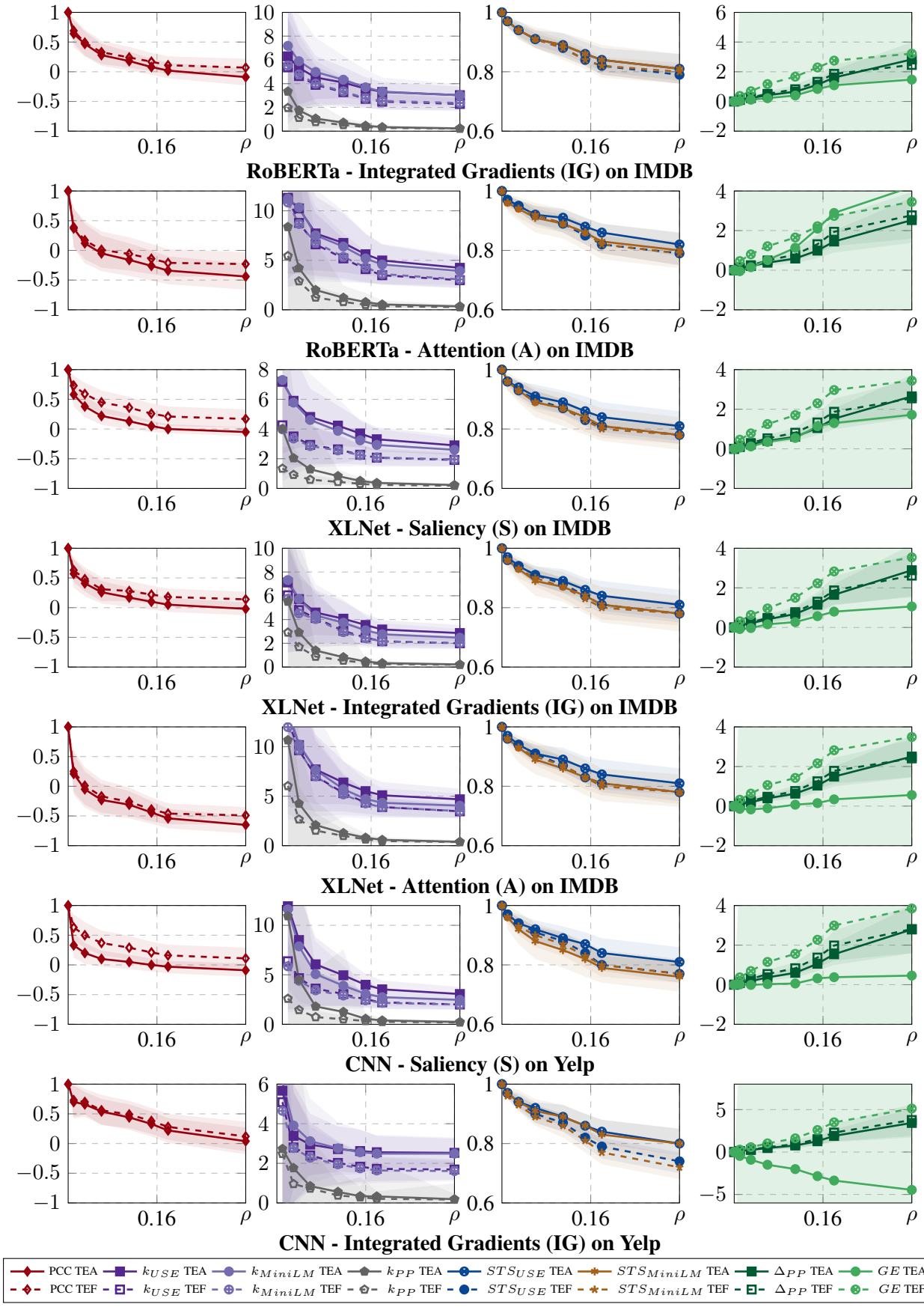

BERT - Saliency (S) on AG's News
BERT - Integrated Gradients (IG) on AG's News
BERT - Attention (A) on AG's News
RoBERTa - Saliency (S) on AG's News
RoBERTa - Integrated Gradients (IG) on AG's News
RoBERTa - Attention (A) on AG's News
XLNet - Saliency (S) on AG's News
PCC TEA
k_{USE} TEA
k_{MiniLM} TEA
k_{PP} TEA
STS_{USE} TEA
STS_{MiniLM} TEA
Δ_{PP} TEA
GE TEA
PCC TEF
k_{USE} TEF
k_{MiniLM} TEF
k_{PP} TEF
STS_{USE} TEF
STS_{MiniLM} TEF
Δ_{PP} TEF
GE TEF

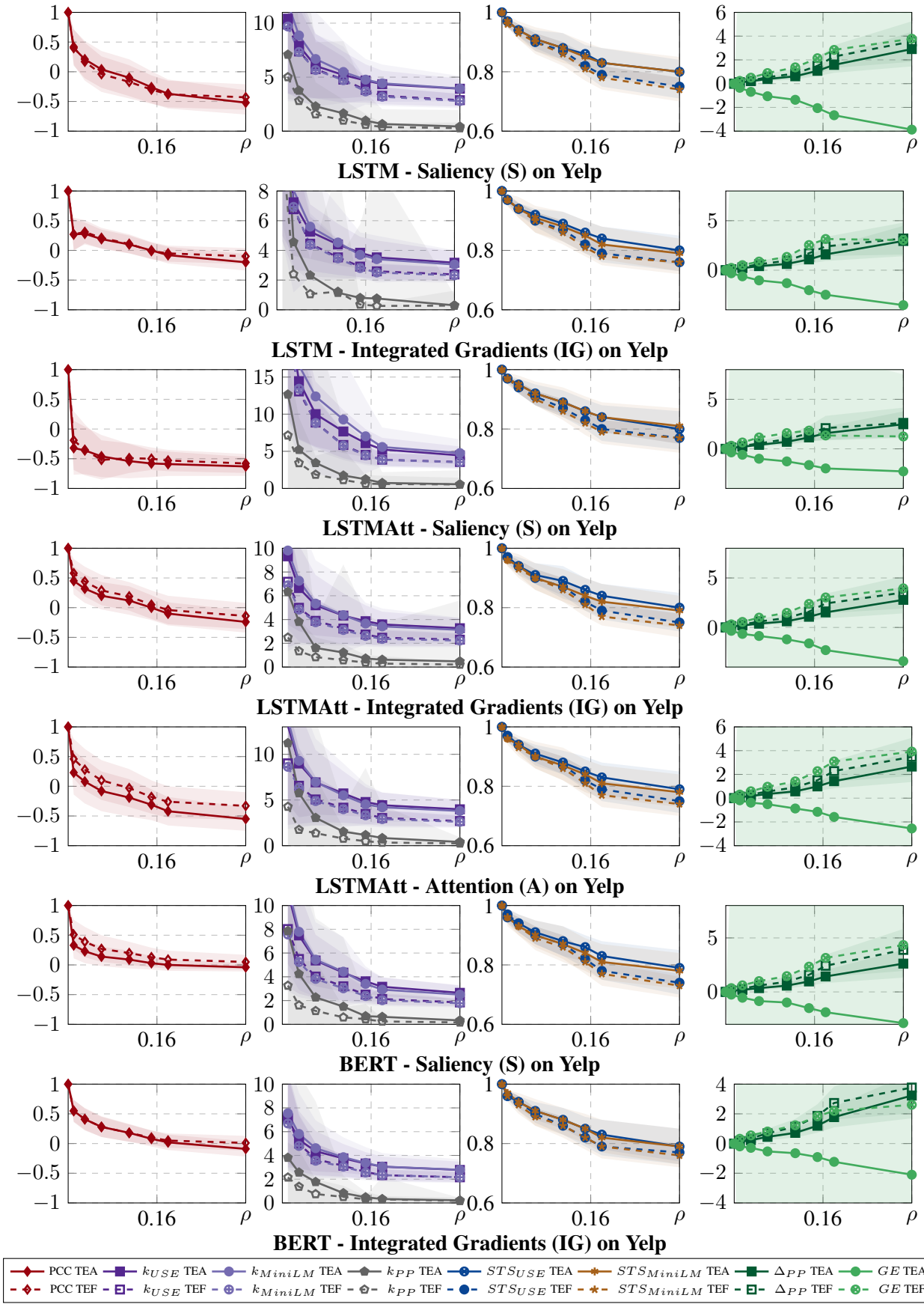

XLNet - Integrated Gradients (IG) on AG's News
XLNet - Attention (A) on AG's News
CNN - Saliency (S) on MR
CNN - Integrated Gradients (IG) on MR
LSTM - Saliency (S) on MR
LSTM - Integrated Gradients (IG) on MR
LSTMAtt - Saliency (S) on MR
PCC TEA
k_{USE} TEA
k_{MiniLM} TEA
k_{PP} TEA
STS_{USE} TEA
STS_{MiniLM} TEA
Δ_{PP} TEA
GE TEA
PCC TEF
k_{USE} TEF
k_{MiniLM} TEF
k_{PP} TEF
STS_{USE} TEF
STS_{MiniLM} TEF
Δ_{PP} TEF
GE TEF

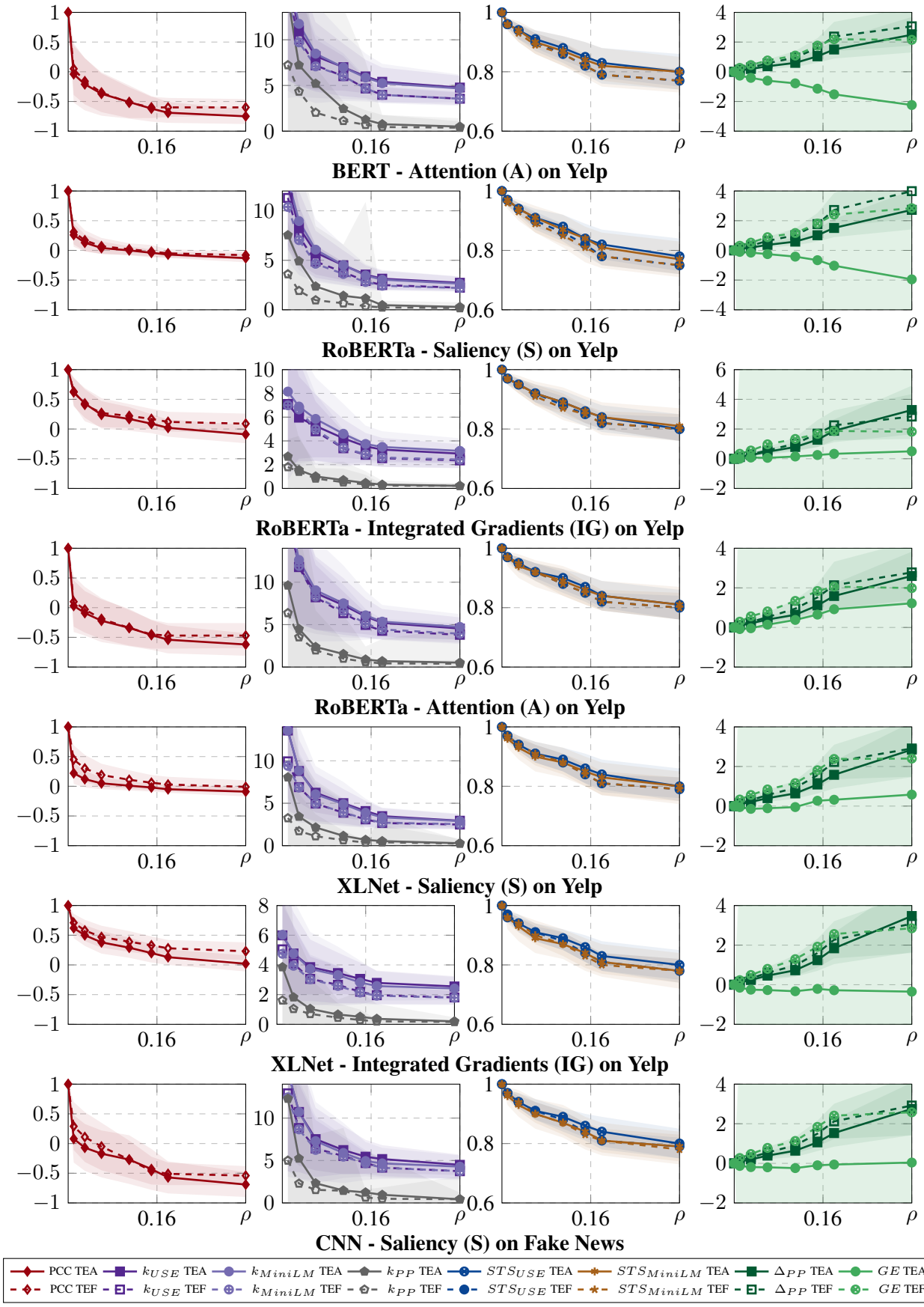

LSTMAtt - Integrated Gradients (IG) on MR
LSTMAtt - Attention (A) on MR
BERT - Saliency (S) on MR
BERT - Integrated Gradients (IG) on MR
BERT - Attention (A) on MR
RoBERTa - Saliency (S) on MR
RoBERTa - Integrated Gradients (IG) on MR
PCC TEA
k_{USE} TEA
k_{MiniLM} TEA
k_{PP} TEA
STS_{USE} TEA
STS_{MiniLM} TEA
Δ_{PP} TEA
GE TEA
PCC TEF
k_{USE} TEF
k_{MiniLM} TEF
k_{PP} TEF
STS_{USE} TEF
STS_{MiniLM} TEF
Δ_{PP} TEF
GE TEF

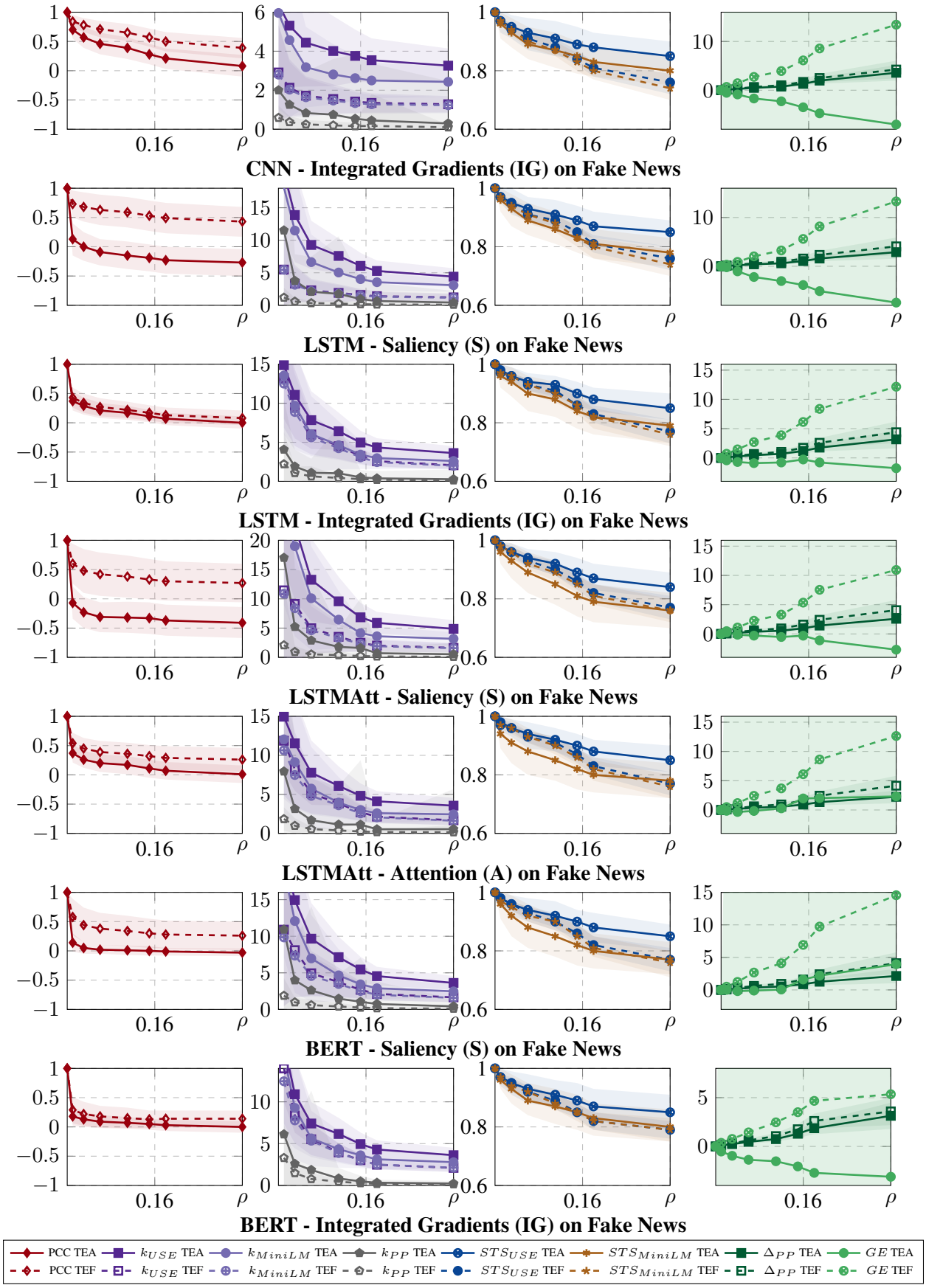

XLNet - Saliency (S) on MR
XLNet - Integrated Gradients (IG) on MR
XLNet - Attention (A) on MR
CNN - Saliency (S) on IMDB
CNN - Integrated Gradients (IG) on IMDB
LSTM - Saliency (S) on IMDB
LSTM - Integrated Gradients (IG) on IMDB
0.16
ρ
PCC TEA
PCC TEF
k_{USE} TEA
k_{USE} TEF
k_{MiniLM} TEA
k_{MiniLM} TEF
k_{PP} TEA
k_{PP} TEF
STS_{USE} TEA
STS_{USE} TEF
STS_{MiniLM} TEA
STS_{MiniLM} TEF
Δ_{PP} TEA
Δ_{PP} TEF
GE TEA
GE TEF

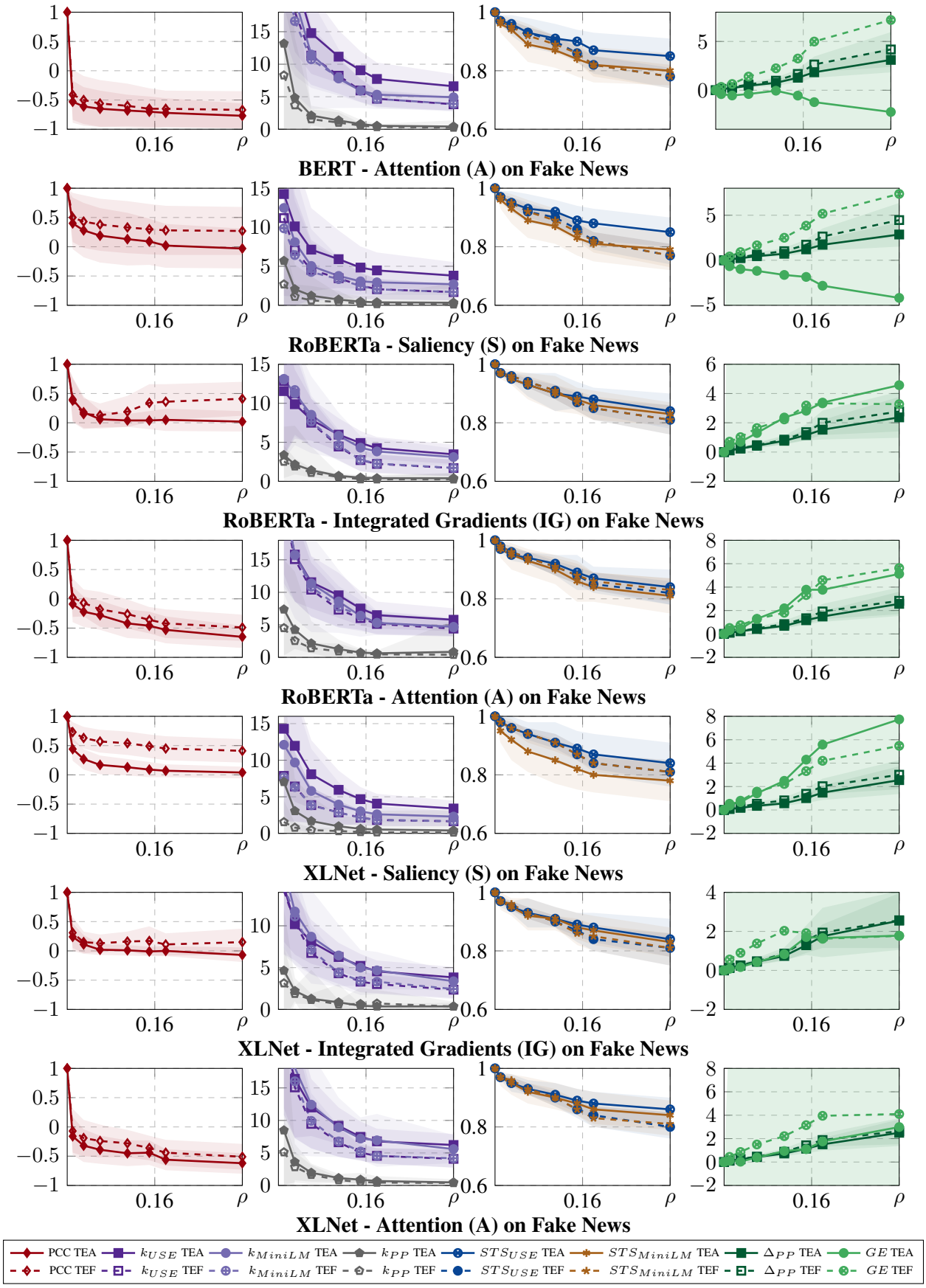

LSTMAtt - Saliency (S) on IMDB
LSTMAtt - Integrated Gradients (IG) on IMDB
LSTMAtt - Attention (A) on IMDB
BERT - Saliency (S) on IMDB
BERT - Integrated Gradients (IG) on IMDB
BERT - Attention (A) on IMDB
RoBERTa - Saliency (S) on IMDB
PCC TEA
k_{USE} TEA
k_{MiniLM} TEA
k_{PP} TEA
STS_{USE} TEA
STS_{MiniLM} TEA
Δ_{PP} TEA
GE TEA
PCC TEF
k_{USE} TEF
k_{MiniLM} TEF
k_{PP} TEF
STS_{USE} TEF
STS_{MiniLM} TEF
Δ_{PP} TEF
GE TEF

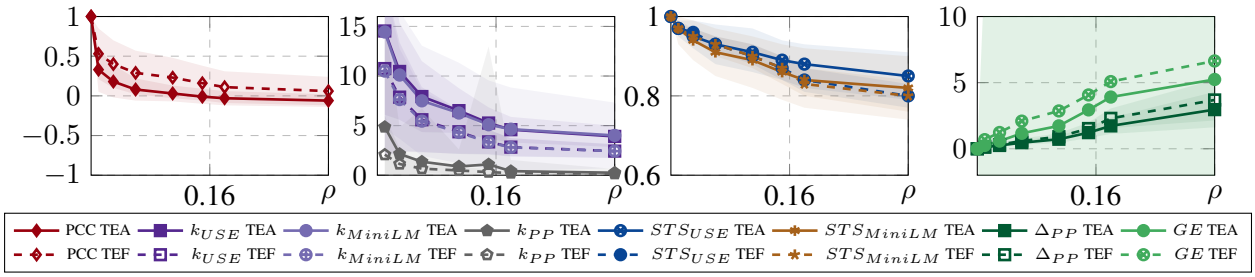

RoBERTa - Integrated Gradients (IG) on IMDB
RoBERTa - Attention (A) on IMDB
XLNet - Saliency (S) on IMDB
XLNet - Integrated Gradients (IG) on IMDB
XLNet - Attention (A) on IMDB
CNN - Saliency (S) on Yelp
CNN - Integrated Gradients (IG) on Yelp
0.16
ρ
PCC TEA
k_{USE} TEA
k_{MiniLM} TEA
k_{PP} TEA
STS_{USE} TEA
STS_{MiniLM} TEA
Δ_{PP} TEA
GE TEA
PCC TEF
k_{USE} TEF
k_{MiniLM} TEF
k_{PP} TEF
STS_{USE} TEF
STS_{MiniLM} TEF
Δ_{PP} TEF
GE TEF


LSTM - Saliency (S) on Yelp
LSTM - Integrated Gradients (IG) on Yelp
LSTMAtt - Saliency (S) on Yelp
LSTMAtt - Integrated Gradients (IG) on Yelp
LSTMAtt - Attention (A) on Yelp
BERT - Saliency (S) on Yelp
BERT - Integrated Gradients (IG) on Yelp
PCC TEA
k_{USE} TEA
k_{MiniLM} TEA
k_{PP} TEA
STS_{USE} TEA
STS_{MiniLM} TEA
Δ_{PP} TEA
GE TEA
PCC TEF
k_{USE} TEF
k_{MiniLM} TEF
k_{PP} TEF
STS_{USE} TEF
STS_{MiniLM} TEF
Δ_{PP} TEF
GE TEF


BERT - Attention (A) on Yelp
RoBERTa - Saliency (S) on Yelp
RoBERTa - Integrated Gradients (IG) on Yelp
RoBERTa - Attention (A) on Yelp
XLNet - Saliency (S) on Yelp
XLNet - Integrated Gradients (IG) on Yelp
CNN - Saliency (S) on Fake News
PCC TEA
k_{USE} TEA
k_{MiniLM} TEA
k_{PP} TEA
STS_{USE} TEA
STS_{MiniLM} TEA
Δ_{PP} TEA
GE TEA
PCC TEF
k_{USE} TEF
k_{MiniLM} TEF
k_{PP} TEF
STS_{USE} TEF
STS_{MiniLM} TEF
Δ_{PP} TEF
GE TEF


CNN - Integrated Gradients (IG) on Fake News
LSTM - Saliency (S) on Fake News
LSTM - Integrated Gradients (IG) on Fake News
LSTMAtt - Saliency (S) on Fake News
LSTMAtt - Attention (A) on Fake News
BERT - Saliency (S) on Fake News
BERT - Integrated Gradients (IG) on Fake News
PCC TEA
k_{USE} TEA
k_{MiniLM} TEA
k_{PP} TEA
STS_{USE} TEA
STS_{MiniLM} TEA
Δ_{PP} TEA
GE TEA
PCC TEF
k_{USE} TEF
k_{MiniLM} TEF
k_{PP} TEF
STS_{USE} TEF
STS_{MiniLM} TEF
Δ_{PP} TEF
GE TEF


BERT - Attention (A) on Fake News
RoBERTa - Saliency (S) on Fake News
RoBERTa - Integrated Gradients (IG) on Fake News
RoBERTa - Attention (A) on Fake News
XLNet - Saliency (S) on Fake News
XLNet - Integrated Gradients (IG) on Fake News
XLNet - Attention (A) on Fake News
PCC TEA
k_{USE} TEA
k_{MiniLM} TEA
k_{PP} TEA
STS_{USE} TEA
STS_{MiniLM} TEA
Δ_{PP} TEA
GE TEA
PCC TEF
k_{USE} TEF
k_{MiniLM} TEF
k_{PP} TEF
STS_{USE} TEF
STS_{MiniLM} TEF
Δ_{PP} TEF
GE TEF


1
0.5
0
−0.5
−1
0.16
ρ
15
10
5
0
0.16
ρ
1
0.8
0.6
0.16
ρ
10
5
0
0.16
ρ
PCC TEA
k_{USE} TEA
k_{MiniLM} TEA
k_{PP} TEA
STS_{USE} TEA
STS_{MiniLM} TEA
Δ_{PP} TEA
GE TEA
PCC TEF
k_{USE} TEF
k_{MiniLM} TEF
k_{PP} TEF
STS_{USE} TEF
STS_{MiniLM} TEF
Δ_{PP} TEF
GE TEF